thus escaped by being carried away rapidly to the surface during the northwest flank dike intrusion, causing the system to be partially degassed beneath the summit caldera. This mechanism is supported by geophysical observations of Usu during the eruption and post-eruption period (3, 4).

References and Notes

1. Y. Oba, *J. Fac. Sci. Hokkaido Univ., Ser. 4* **13**, 185 (1966).
2. I. Yokoyama, M. Seino, *Earth Planets Space* **52**, 73 (2000).
3. Smithsonian Institution, *Bull. Global Volcanism Network* **25** (no. 3), 2 (2000).
4. ———, *Bull. Global Volcanism Network* **25** (no. 6), 2 (2000).
5. J. Carbonnelle, P. Zetwoog, *Bull. PIRPSEV-CNRS* **55**, 15 pp. (1982).
6. L. P. Greenland *et al.*, *Geochim. Cosmochim. Acta* **49**, 125 (1985).
7. T. M. Gerlach, E. J. Graeber, *Nature* **313**, 273 (1986).
8. J. W. Hedenquist, *Report 279* (Geological Survey of Japan, Ibaraki, 1992).
9. G. Chiodini *et al.*, *Appl. Geochem.* **13**, 543 (1998).
10. J. C. Baubron, R. Mathieu, G. Miele, in *Napoli'91, International Conference on Active Volcanoes and Risk Mitigation, Abstracts* (Osservatorio Vesuviano, Napoli, Italy, 1991).
11. K. J. Parkinson, *J. Appl. Ecol.* **18**, 221 (1981).
12. N. A. C. Cressie, *Math. Geol.* **22**, 239 (1990).
13. A. Journel, in *Principles of Environment Sampling*, L. Keith, Ed. (American Chemical Society, Washington, DC, 1988), pp. 45–72.
14. J. C. Baubron, P. Allard, J.-C. Sabroux, D. Tedesco, J.-P. Toutain, *J. Geol. Soc. London* **148**, 571 (1991).
15. G. Chiodini, F. Frondini, B. Raco, *Bull. Volcanol.* **58**, 41 (1996).
16. J. C. Baubron, P. Allard, J. P. Toutain, *Nature* **344**, 51 (1990).
17. A. J. Sinclair, *J. Geochem. Explor.* **3**, 129 (1974).
18. W. F. Giggenbach, S. Matsuo, *Appl. Geochem.* **6**, 125 (1991).
19. Y. Sano, H. Wakita, *J. Geophys. Res.* **90**, 8729 (1985).
20. P. Allard *et al.*, *Nature* **351**, 387 (1991).
21. H. L. Penman, *J. Agric. Sci.* **30**, 437 (1940).
22. S.-H. Lai *et al.*, *Soil Sci. Soc. Am. J.* **40**, 3 (1976).
23. T. M. Gerlach *et al.*, *Geophys. Res. Lett.* **25**, 1947 (1998).
24. We are grateful to P. Quintero and A. Martinez for their help in the field and for their laboratory work and M. Sohirad for help with English. Helpful review of the manuscript was provided by K. Nagao and D. López. We are indebted to the staff of the Usu Volcano Observatory for their assistance during the surveys. This research was supported by grants from the Japan Society for the Promotion of Science, Cabildo Insular de Tenerife (Canary Islands, Spain), and the European Union.

Control of Nitrogen Export from Watersheds by Headwater Streams

Bruce J. Peterson,[1] Wilfred M. Wollheim,[1] Patrick J. Mulholland,[2] Jackson R. Webster,[3] Judy L. Meyer,[4] Jennifer L. Tank,[5] Eugènia Martí,[6] William B. Bowden,[7] H. Maurice Valett,[3] Anne E. Hershey,[8] William H. McDowell,[9] Walter K. Dodds,[10] Stephen K. Hamilton,[11] Stanley Gregory,[12] Donna D. Morrall[13]

A comparative ^{15}N-tracer study of nitrogen dynamics in headwater streams from biomes throughout North America demonstrates that streams exert control over nutrient exports to rivers, lakes, and estuaries. The most rapid uptake and transformation of inorganic nitrogen occurred in the smallest streams. Ammonium entering these streams was removed from the water within a few tens to hundreds of meters. Nitrate was also removed from stream water but traveled a distance 5 to 10 times as long, on average, as ammonium. Despite low ammonium concentration in stream water, nitrification rates were high, indicating that small streams are potentially important sources of atmospheric nitrous oxide. During seasons of high biological activity, the reaches of headwater streams typically export downstream less than half of the input of dissolved inorganic nitrogen from their watersheds.

Nitrogen (N) loading of terrestrial and aquatic ecosystems is increasing worldwide as a result of human activities such as fertilizer application, N fixation by legume crops, human and animal waste disposal, and fossil fuel combustion (1). As terrestrial ecosystems become saturated with N (2), excess N moves with surface runoff and groundwater flow to streams, lakes, rivers, and coastal oceans (3, 4). Because streams transport much of this N, quantitative information on N cycling in streams is needed to understand how N loading from watersheds will affect rivers, lakes, and estuaries where N availability can limit primary production (5, 6). Results from this cross-site tracer study of stream N cycling demonstrate how watershed-derived N is processed in stream channels and how these transformations affect the export of N to downstream ecosystems.

Headwater streams convey water and nutrients to larger streams and, despite their relatively small dimensions, play a disproportionately large role in N transformations on the landscape. Small streams (width 10 m or less) often constitute up to 85% of total stream length within a drainage network (7, 8) and collect most of the water and dissolved nutrients from adjacent terrestrial ecosystems. Nitrogen in small streams has been intensively monitored in watershed nutrient budget studies (9–12), and data on N transport in rivers suggest that the smaller streams and rivers are most effective in N processing and retention in large watersheds (13). However, the dynamics of N cycling within stream channels have remained obscure because of a lack of techniques for tracing the fluxes of N at ambient concentrations.

Here, we report on rates of N uptake, storage, regeneration, and export in headwater streams. These processes were assessed via standardized protocols (14) in 12 headwater streams as part of the Lotic Intersite Nitrogen eXperiment (LINX). These streams and their watersheds (i.e., catchments) represent a diversity of biomes throughout the United States [Fig. 1; see Web table 1 (15)]. With only two exceptions, the streams had relatively low inorganic N levels (<10 μg NH_4-N liter^{-1}). Each experiment involved a 6-week continuous tracer-level addition of a stable N isotope as [^{15}N]NH_4 to each stream (15). Sampling was designed to measure ^{15}N tracer movement through biotic and abiotic components of each stream during and for several weeks after tracer addition (15).

Cross-site comparison of NH_4 uptake lengths (16) revealed that the distance trav-

[1]Ecosystems Center, Marine Biological Laboratory, Woods Hole, MA 02543, USA. [2]Environmental Sciences Division, Oak Ridge National Laboratory, Post Office Box 2008, Oak Ridge, TN 37831, USA. [3]Department of Biology, Virginia Polytechnic Institute and State University, Blacksburg, VA 24061, USA. [4]Institute of Ecology, University of Georgia, Athens, GA 30602, USA. [5]Department of Natural Resources and Environmental Sciences, University of Illinois, N-411 Turner Hall, 1102 South Goodwin Avenue, Urbana, IL 61801, USA. [6]Centre d'Estudis Avancats de Blanes, Cami de Sta. Barbara s/n, 17300 Blanes, Girona, Spain. [7]Landcare Research, Post Office Box 69, Lincoln 8152, New Zealand. [8]Department of Biology, University of North Carolina, Greensboro, NC 27402, USA. [9]Department of Natural Resources, University of New Hampshire, James Hall, Durham, NH 03824, USA. [10]Division of Biology, Kansas State University, 232 Ackert Hall, Manhattan, KS 66506, USA. [11]Kellogg Biological Station, Michigan State University, Hickory Corners, MI 49060, USA. [12]Department of Fisheries and Wildlife, Oregon State University, Corvallis, OR 97331, USA. [13]Procter & Gamble Company, Experimental Stream Facility, 1003 Route 50, Milford, OH 45150, USA.

eled by NH_4 molecules was strongly correlated with stream discharge, even across this wide range of biomes (Fig. 2). In headwater streams, uptake and removal processes occur mainly on sediments and biofilms covering submerged surfaces. Thus, the shallow depths and high surface-to-volume ratios characteristic of the smaller streams largely account for their short uptake lengths relative to larger streams (17). Most of the variation in uptake length among streams was attributable to differences in physical characteristics such as depth and current velocity, which correlate with discharge. But the residual variation in ammonium uptake length was due to differences in rates of uptake processes.

The mass transfer coefficient v_f (18) is a measure of NH_4 uptake rate, relative to availability in the water, that normalizes for physical effects of varying stream depth and current velocity. LINX streams ranged over only one order of magnitude in v_f, from about 0.3×10^{-4} to 7.0×10^{-4} m s^{-1} (Fig. 3A). Similarly the rate of NH_4 uptake (μg m^{-2} s^{-1}) varied by an order of magnitude (Fig. 3B). Because the range in discharge among study streams varied over several orders of magnitude while v_f values varied much less as stream size increased, hydrological influences of stream depth and current velocity were the primary determinants of NH_4 uptake length.

NH_4 was removed from stream water primarily through assimilation by photosynthetic (unicellular algae, filamentous algae, and bryophytes) and heterotrophic (bacteria and fungi) organisms and by sorption to sediments (19), and secondarily by nitrification. Nitrification varied widely, from less than 3% of NH_4 removal (southern deciduous forest stream in North Carolina) to 60% (tropical rainforest stream in Puerto Rico) (Fig. 3B) (15). On average, 70 to 80% of NH_4 removal was due to uptake on the stream bottom, and 20 to 30% was due to nitrification. Streams with high nitrification rates tended to have high NO_3 concentrations, which suggests that nitrification in stream channels as well as terrestrial NO_3 inputs affect stream NO_3 concentrations (20).

Nitrate was removed from stream water by biological assimilation and denitrification processes. The areal rate of NO_3 uptake (μg N m^{-2} s^{-1}) in LINX streams was on average about equal to NH_4 uptake (Fig. 3C), even though NO_3 concentrations averaged about an order of magnitude greater than NH_4 concentrations in these streams [Web table 1 (15)]. Thus, NO_3 molecules traveled on average about 10 times as far as NH_4 molecules.

One day after stopping the ^{15}N tracer addition, we measured rates of [^{15}N]NH_4 and [^{15}N]NO_3 release from the stream bottom at each site to determine how rapidly the ^{15}N stored on the stream bottom was being re-

turned to the water [i.e., the rate of inorganic N regeneration (15)]. The rate of [^{15}N]NH_4 plus [^{15}N]NO_3 regeneration ranged from undetectable to 63% of the prior tracer addition rate (Fig. 3D), indicating that N fluxes from the stream bottom back to the water were also important in determining inorganic N concentrations. Because experiments were done during periods of relatively high biotic activity, excesses of inorganic N removal over regeneration were expected. However, over annual cycles, stream channels do not normally accumulate nutrient or organic matter stocks, and consequently most of this stored N will ultimately be exported as regenerated inorganic, gaseous, or organic N within a period ranging from weeks to several years (21, 22).

The emergent general pattern of N cycling in these headwater streams is summarized in Fig. 4. NH_4 entering the streams is rapidly removed from the water by biological assimilation, sorption, and nitrification. Inputs of NO_3 are removed on average less efficiently. NH_4 concentrations are typically lower than NO_3 concentrations because NO_3 inputs are often higher than NH_4 inputs, NH_4 sorbs more readily to sediments, NH_4 assimilation is energetically preferable to NO_3 assimilation (23), and NH_4 is rapidly nitrified. The NO_3 and NH_4 sequestered as sorbed and organic N on stream bottoms turn over on time scales of weeks to months with a release of important amounts of NH_4 and NO_3 back to the stream water.

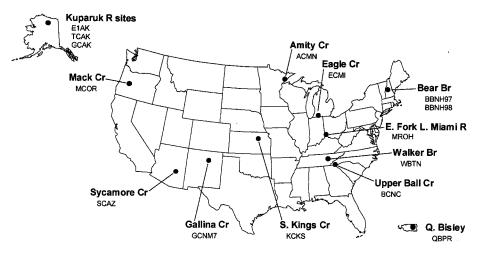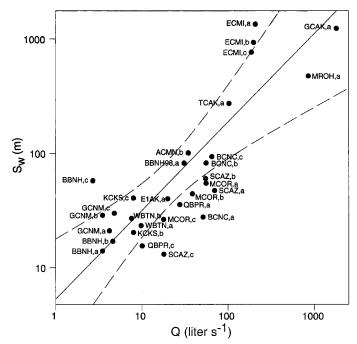Frequently these input and removal pro-

Fig. 1. Location of the LINX study streams. Letters below stream names indicate codes for streams and locations (e.g., BBNH = Bear Brook, New Hampshire). See Web table 1 (15).

Fig. 2. Relation between stream discharge (Q) and NH_4 uptake length (S_w) for the LINX streams. Stream points are abbreviated by name and state; see Web table 1 (15) for full stream names. Letters next to abbreviations refer to date of sampling: a = day 0, b = day 20, and c = day 41 (or day 35 for KCKS). NH_4-S_w in BBNH was also determined in summer 1998 during a second ^{15}N addition and is denoted by BBNH98. The solid line is the regression; dashed lines are the 95% confidence interval (CI) of the relation for all points. The regression equation is $\log(NH_4$-$S_w) = 0.71 \log(Q) + 0.78$ ($r^2 = 0.71$, $n = 30$, $P < 0.01$).

cesses are balanced, such that NH_4 and NO_3 concentrations in streams exhibit only slight variation with distance [but see (24)]. Constant longitudinal concentration profiles have been interpreted to indicate that stream channels are relatively unreactive conduits with nutrient levels determined solely by terrestrial inputs, but our study and others suggest otherwise (13, 21, 22, 25–29). We find that NH_4 and NO_3 in streams are in dynamic balance, controlled by input, nitrification, biological uptake, sorption, and regeneration.

To illustrate the impact of stream channel processes on inorganic N export from small watersheds, we computed how N processing rates measured in LINX streams (data from Fig. 3) would alter NO_3 and NH_4 concentrations of headwater spring and lateral seepage inputs by the time water in a headwater stream channel passed a monitoring station located 1 km downstream (15) (Fig. 5). We chose input nitrogen concentrations in the spring and in seepage inputs distributed along the entire stream channel of 20 μg N liter^{-1} for NH_4 and 50 μg N liter^{-1} for NO_3 (Fig. 5); these values are reasonable considering ambient concentrations in LINX streams [Web table 1 (15)].

When rates of stream N processing were set to match the average NH_4 and NO_3 kinetics measured in LINX streams (Fig. 5, scenario 1), the 1-km reach retained 64% of DIN (dissolved inorganic nitrogen; sum of NH_4 and NO_3) inputs from land and exported the remaining 36% downstream. NH_4 and NO_3 concentrations were much reduced at the downstream end of the reach (2.7 and 20.6 μg liter^{-1}, respectively). The higher concentration of NO_3 versus NH_4 at 1 km resulted from a combination of higher NO_3 input, production of NO_3 in the stream via nitrification, and the longer uptake distance for NO_3 compared to NH_4.

To illustrate the consequences of the variability in N cycle process rates among LINX streams, we evaluated a series of alternative N processing scenarios consistent with the range of measured uptake, nitrification, and stream bottom regeneration rates. Stream water chemistry at the 1-km monitoring site under all scenarios reflected both DIN concentrations in seepage inputs and changes caused by stream processes. Model scenarios 2 and 3 compared low versus high NH_4 uptake rates (Fig. 5). The measured range of NH_4 uptake rates was relatively small, and thus downstream DIN concentration varied only 6%. However, when NH_4 uptake was arbitrarily set to zero, DIN retention fell to only 35% of inputs (scenario not shown). Changing the nitrification rate from undetectable to the highest measured (scenarios 4 and 5, respectively) increased NO_3 concentration in the stream and increased DIN export by 8%. If NO_3 uptake was set to zero (scenario 6), stream

water NO_3 concentrations were even greater than in seepage inputs due to nitrification, and DIN retention fell to 15%. High NO_3 uptake, on the other hand, resulted in an estimated retention of 87% of DIN inputs (scenario 7). Inorganic N regeneration from the stream bottom varied from below detection to 63% of DIN uptake (Fig. 3D); DIN retention was 72% with zero regeneration and 51% with high regeneration (scenarios 8 and 9). In all scenarios in Fig. 5, NO_3 input concentrations were 2.5 times NH_4 concentrations. Unless NH_4 or NO_3 uptake was unusually low, the model scenarios estimated 60 to 70% retention of DIN inputs. Retention would be even greater if seepage inputs were dominated by NH_4 because of the higher mass transfer coefficients for NH_4 than for NO_3.

Headwater streams retain and transform important amounts of inorganic N, frequently more than 50% of the inputs from their watersheds. It is probable that low to moderate inorganic N inputs to headwater streams will be removed or transformed within minutes to hours and within a few tens to hundreds of

meters. In larger streams, the times and distances increase in proportion to depth (13, 17) or discharge (30) (Fig. 2). During transit from uplands to oceans via the stream network, most inorganic N inputs to headwater streams will undergo multiple cycles of uptake, storage, and regeneration, referred to as spiraling (31, 32). Repeated cycles of nitrification, stream bottom N uptake, and regeneration set the stage for NO_3 removal by denitrification and for production of the greenhouse gas N_2O during redox transformations occurring during both nitrification and denitrification processes (33).

As N inputs to streams increase, the capacity of streams to effectively retain and transform nitrogen inputs will be overwhelmed (30) and inorganic N will be transported much farther, with consequent increases in eutrophication of rivers, lakes, and estuaries. The small-size streams may be the most important in regulating water chemistry in large drainages because their large surface-to-volume ratios favor rapid N uptake and processing (Fig. 2). Yet small streams are
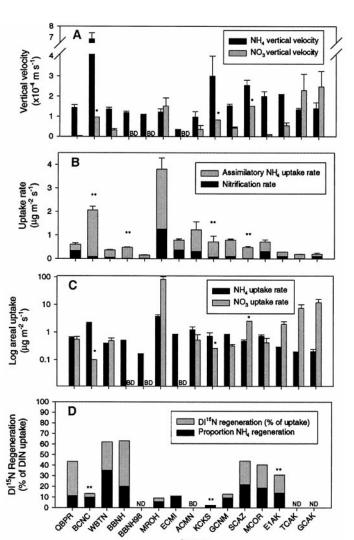

Fig. 3. Site-specific rates of N cycling in LINX streams. (**A**) Mass transfer coefficients for NH_4 and NO_3. (**B**) Rates of NH_4 removal and direct nitrification. (**C**) Rates of NO_3 uptake compared to NH_4 uptake. (**D**) Rates of inorganic N regeneration from the stream bottom, expressed as a percentage of the ^{15}N addition rate. Error bars refer to 95% CI. Symbols: *, a minimum estimate of NO_3 mass transfer coefficient (v_f) and uptake and a maximum estimate of nitrification; **, nitrification or regeneration estimates that are likely maxima because of low ^{15}N enrichments; BD, below detection; ND, no data.

endangered because they are the most vulnerable to human disturbance, such as diversion, channelization, and elimination in agricultural and urban environments (*34*). Restoration and preservation of small stream ecosystems should be a central focus of management strategies to ensure maximum N processing in watersheds, which in turn will improve the quality of water delivered to downstream lakes, estuaries, and oceans.
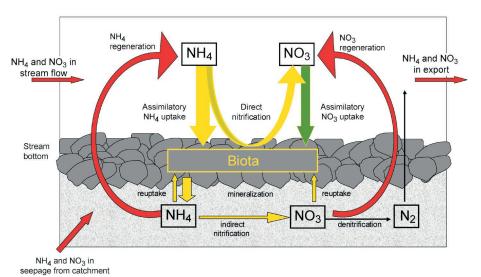

Fig. 4. Conceptual model of DIN dynamics in headwater stream ecosystems. NH_4 and NO_3 enter the stream reach via stream flow and lateral seepage. NH_4 removal is due to uptake by primary producers, bacteria, and fungi plus direct nitrification. Indirect nitrification is the conversion of NH_4 mineralized from organic matter to NO_3. NO_3 removal from the water is primarily via assimilation by biota and denitrification on the channel bottom. Regeneration is the release of NH_4 and NO_3 from the stream bottom back to the water column and is the net result of several interacting processes, including mineralization, indirect nitrification, denitrification, and reuptake by organisms. NO_3 and NH_4 remaining in the water are exported downstream.
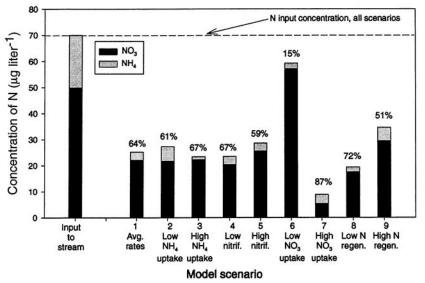

Fig. 5. Model scenarios of the impact of stream N cycle processes on spring and seepage water chemistry within the first kilometer of flow in a headwater stream (*15*). The leftmost bar represents the inorganic N composition of groundwater entering the stream via the spring and laterally via seepage along the entire channel length. Remaining bars show predicted stream water chemistry at 1 km from the stream origin for scenarios where NH_4 and NO_3 removal, nitrification, storage, and regeneration rates are constrained to be within the ranges of measured rates in LINX streams. Scenario 1 is based on the mean N process rates measured across all LINX streams. All subsequent scenarios vary only one rate at a time from scenario 1. The percentages associated with each scenario are the calculated retention of inorganic N by the stream ecosystem. Scenarios 2 and 3 compare low versus high NH_4 uptake rate, scenarios 4 and 5 compare low versus high nitrification rate, scenarios 6 and 7 compare zero versus high NO_3 uptake rate, and scenarios 8 and 9 compare low versus high inorganic N regeneration rates.

References and Notes

1. P. M. Vitousek *et al.*, *Ecol. Appl.* **7**, 737 (1997).
2. J. Aber *et al.*, *Bioscience* **48**, 921 (1998).
3. B. J. Peterson, J. M. Melillo, *Tellus* **37**, 117 (1985).
4. T. E. Jordan, D. E. Weller, *Bioscience* **46**, 655 (1996).
5. J. J. Elser, E. R. Marzolf, C. R. Goldman, *Can. J. Fish. Aquat. Sci.* **47**, 1468 (1990).
6. C. S. Hopkinson, J. J. Vallino, *Estuaries* **18**, 598 (1995).
7. R. J. Naiman, in *Periphyton of Freshwater Ecosystems*, R. Wetzel, Ed. (Junk, The Hague, 1983), pp. 191–198.
8. R. E. Horton, *Bull. Geol. Soc. Am.* **56**, 275 (1945).
9. F. H. Bormann, G. E. Likens, D. W. Fisher, R. S. Pierce, *Science* **159**, 882 (1968).
10. K. J. Nadelhoffer, M. Downs, B. Fry, A. Magill, J. D. Aber, *Env. Monitor. Assess.* **55**, 187 (1999).
11. G. E. Likens, F. H. Bormann, N. M. Johnson, D. W. Fisher, R. S. Pierce, *Ecol. Monogr.* **40**, 23 (1970).
12. G. M. Lovett, K. C. Weathers, W. V. Sobczak, *Ecol. Appl.* **10**, 73 (2000).
13. R. B. Alexander, R. A. Smith, G. E. Schwarz, *Nature* **403**, 758 (2000).
14. Identical protocols were followed for experimental design and measurement of hydraulic parameters, nutrients, stream metabolism, N mass distribution in biological and detrital compartments, and stable isotope ratios at all sites. All NH_4 and NO_3 concentrations are given in μg of N (e.g., NH_4-N). NO_3 concentrations include nitrite (NO_2), which occurs in very low concentrations in these streams.
15. For supplementary material on stream sites, isotope additions, stream sampling, calculation of nitrification and NO_3 uptake, calculation of inorganic N regeneration, and the N model, see *Science* Online (www.sciencemag.org/cgi/content/full/292/5514/86/DC1).
16. Ammonium uptake length (NH_4-S_w) is the average downstream distance traveled by NH_4 molecules before removal from the water (*32*). Thus, for any given discharge and NH_4 concentration, a relatively short uptake length indicates a high NH_4 uptake rate, and vice versa. NH_4 uptake length was calculated from the rate of decline of $[^{15}N]NH_4$ flux (μg ^{15}N s^{-1}) over distance downstream of the addition site. $[^{15}N]NH_4$ flux at each station was determined from the $\delta^{15}N$ value, NH_4 concentration, and discharge at each station. S_w was determined from the negative inverse of the slope of natural log–transformed, background-corrected $[^{15}N]NH_4$ flux values versus distance $[S_w = -1/k_1$, where k_1 is the distance-specific uptake rate (m^{-1})].
17. Stream Solute Workshop, *J. N. Am. Benthol. Soc.* **9**, 95 (1990).
18. The mass transfer coefficient v_f is the velocity (m s^{-1}) at which a nutrient molecule moves from the water column to the stream bottom as a result of biological demand or sorption processes: $v_f = (v \times h)/S_w$, where v = water velocity (m s^{-1}), h = water depth (m), and S_w = uptake length (m). Areal uptake rate (U, μg m^{-2} s^{-1}) was determined by $U = v_f \times C$, where C is the ambient nutrient concentration.
19. Retention of NH_4 on the stream bottom may occur through biological processes of assimilation by organisms (*25*) as well as through physical sorption onto fine sediments or organic detritus (*35*). These two processes also may interact, as when adsorbed NH_4 is taken up by microorganisms. The rate of $[^{15}N]NH_4$ removal measured in this study was the sum of both processes. However, because the ^{15}N addition did not change the NH_4 concentration and isotopic equilibration with sorbed NH_4 would occur in minutes to hours, we expect that most removal during the 6-week experiment was due to biological processes.
20. The relation between nitrification rate and nitrate concentration was $\log[NO_3] = 0.72 \times \log(\text{nitrification rate}) + 2.23$ ($r^2 = 0.5$, $n = 10$).
21. B. J. Peterson, M. Bahr, G. W. Kling, *Can. J. Fish. Aquat. Sci.* **54**, 2361 (1997).
22. P. L. Mulholland *et al.*, *Ecol. Monogr.* **70**, 471 (2000).
23. W. K. Dodds, J. C. Priscu, B. K. Ellis, *J. Plankton Res.* **13**, 1339 (1991).
24. L. Dent, N. C. Grimm, *Ecology* **80**, 2283 (1999). Natural features of water and nutrient flow paths in the riparian and hyporheic zones of streams can

25. J. D. Newbold, J. W. Elwood, M. S. Schulze, R. W. Stark, J. C. Barmeir, *Freshwater Biol.* **13**, 193 (1983).
26. P. J. Mulholland *et al.*, *Verh. Internat. Verein. Limnol.*, in press.
27. W. K. Dodds *et al.*, *Ecosystems*, in press.
28. S. K. Hamilton *et al.*, *Biogeochemistry*, in press.
29. J. L. Tank *et al.*, *Limnol. Oceanogr.* **45**, 1013 (2000).
30. W. M. Wollheim *et al.*, *Limnol. Oceanogr.* **46**, 1 (2001).
31. J. R. Webster, B. C. Patten, *Ecol. Monogr.* **49**, 51 (1979).
32. J. D. Newbold, J. W. Elwood, R. V. O'Neill, W. Van Winkle, *Can. J. Fish. Aquat. Sci.* **38**, 860 (1981).
33. S. P. Seitzinger, C. Kroeze, *Global Biogeochem. Cycles* **12**, 93 (1998).
34. J. L. Meyer, J. B. Wallace, in *Ecology: Achievement and Challenge*, M. C. Press, N. Huntly, S. Levin, Eds. (Blackwell Science, Oxford, 2001), pp. 295–317.
35. F. J. Triska, A. P. Jackman, J. H. Duff, R. J. Avanzino, *Biogeochemistry* **26**, 67 (1994).
36. This work is supported by NSF grants DEB-9628860, DEB-9810222, and OPP-9615949. More than 100 students and scientists gathered the information for this synthesis paper. We especially thank S. Johnson, L. Ashkenas, N. Grimm, S. Fisher, C. Dahm, K. Renzanka, J. Merriam, S. Findlay, C. Fellows, R. Hall, R. Holmes, C. Rensha, D. Sanzone, K. MacNeale, and E. Bernhardt for fieldwork, laboratory analyses, and discussion. K. Tholke performed all isotopic analyses.

Tropical Origins for Recent North Atlantic Climate Change

Martin P. Hoerling,[1] James W. Hurrell,[2] Taiyi Xu[1]

Evidence is presented that North Atlantic climate change since 1950 is linked to a progressive warming of tropical sea surface temperatures, especially over the Indian and Pacific Oceans. The ocean changes alter the pattern and magnitude of tropical rainfall and atmospheric heating, the atmospheric response to which includes the spatial structure of the North Atlantic Oscillation (NAO). The slow, tropical ocean warming has thus forced a commensurate trend toward one extreme phase of the NAO during the past half-century.

Large changes in the climate of the extratropical North Atlantic have occurred since 1950. Decadal variations, superimposed on a trend, are especially evident in the leading spatial structure of variability in atmospheric pressure (Fig. 1), known as the NAO. The trend toward its positive phase is described by a strengthening of the middle latitude westerly flow with anomalously low (high) pressure over the subpolar (subtropical) North Atlantic from the surface into the stratosphere (*1*, *2*). This change in atmospheric circulation has contributed substantially to the observed surface warming of the Northern Hemisphere (NH) in recent decades (*1*–*3*), coherent large-scale changes in precipitation over Europe and the Middle East (*1*, *2*), and important changes in both terrestrial and marine ecosystems (*4*, *5*). Yet in spite of these large impacts, the physical mechanisms that govern these decadal and longer term atmospheric variations are poorly understood. We present evidence that concomitant changes in rainfall and atmospheric heating, associated with the progressive warming of the equatorial oceans, have played a central role in producing the observed climate changes over the North Atlantic.

It is well established that much of the atmospheric circulation variability in the form of the NAO arises from processes internal to the atmosphere. For instance, the observed spatial pattern and amplitude of the NAO (Fig. 1) are typically well simulated in atmospheric general circulation models (AGCMs) forced with fixed climatological annual cycles of solar insolation and sea surface temperature (SST), as well as fixed atmospheric trace gas composition (*6*, *7*). Such variability exhibits little temporal coherence, and it has been argued that the observed NAO time series cannot be easily distinguished from a random stationary process (*8*). A possible exception to this interpretation is the strong trend toward the positive index polarity of the NAO over the past 50 years (Fig. 1). Multi-century climate simulations with fixed climatological forcing, for example, do not reproduce North Atlantic interdecadal changes that compare in magnitude to those recently observed (*9*). One possibility, therefore, is that slow changes in the state of the world oceans are necessary conditions for forcing the North Atlantic atmosphere on these longer time scales.

Evidence for this viewpoint comes from ensemble AGCM experiments where the model is forced with the known global evolution of SST and sea ice concentrations over the past 50 years (*10*, *11*). One example of such a Global Ocean Global Atmosphere (GOGA) result is shown in the lower panel of Fig. 1 (*12*). It is clear that the low-frequency behavior in the simulated NAO time series, including an overall upward trend, closely resembles the observations. Indeed, the two filtered atmospheric time series (Fig. 1) are significantly correlated at 0.8 (*13*). This confirms the results of earlier GOGA ensemble experiments performed with different AGCMs

and indicates that North Atlantic climate variability is not merely stochastic atmospheric noise, but rather contains a component that is a response to changes in ocean surface temperatures and/or sea ice (*10*, *11*). But what portion of the world oceans is driving the North Atlantic atmosphere?

One working hypothesis has been that the North Atlantic basin itself is the most relevant (*10*, *14*, *15*). A key and long-standing issue in this regard, however, has been the extent to which anomalous extratropical SST and upper ocean heat content anomalies feed back to affect the atmosphere. Most evidence suggests this effect is quite small on interannual time scales compared with internal atmospheric variability (*16*).

Another possibility is that changes in tropical heating force a remote atmospheric response over the North Atlantic that, in turn, drives changes in extratropical SSTs and sea ice. Simple linear regressions between global SSTs and the low-frequency observed and simulated NAO time series during boreal winter suggests the recent North Atlantic climate changes might originate from the tropics (Fig. 2). The regressions reveal a coherent pattern of tropic-wide warm SSTs associated with the positive NAO phase. In fact, the tropical loadings resemble the pattern of SST trend since 1950, the principal feature of which is a warming of Indo-Pacific waters (*17*).

To isolate the role of changes in tropical SSTs, another ensemble of simulations was performed. In these experiments, the time history of observed SSTs was specified over tropical latitudes (30°S to 30°N) since 1950, but the AGCM was forced by a repeating annual cycle of monthly climatological values of SST and sea ice at higher latitudes (*18*). These experiments are known as Tropical Ocean Global Atmosphere (TOGA) integrations. The observed wintertime trends in Northern Hemisphere 500 hPa height are contrasted with those from the GOGA and TOGA simulations in Fig. 3.

It is evident that the observed NAO trend is part of a hemisphere-wide change in circulation that is also characterized by lower heights over the central North Pacific and higher heights over western Canada. The GOGA ensemble reproduces the spatial pattern of the trend remarkably well, but perhaps most striking is that

[1]Climate Diagnostics Center, National Oceanic and Atmospheric Administration–Environmental Research Laboratories, Boulder, CO 80303, USA. [2]National Center for Atmospheric Research, Post Office Box 3000, Boulder, CO 80307, USA.

To whom correspondence should be addressed. E-mail: mph@cdc.noaa.gov